Advances in Continuous and Discrete Models

RESEARCH Open Access

Analysis of Huanglongbing transmission model with vector preferences and heterogeneous environments

Youquan Luo[1], Shuimei Tang[1], Fumin Zhang[1], Yujiang Liu[1] and Shujing Gao[1,2*]

*Correspondence:
gaosjmath@126.com
[1]Jiangxi Provincial Key Laboratory of Pest and Disease Control of Featured Horticultural Plants, Gannan Normal University, Ganzhou, 341000, P.R. China
[2]National Navel Orange Engineering Research Center, Gannan Normal University, Ganzhou, 341000, P.R. China

Abstract

The world citrus industry is confronting an unprecedented challenge from citrus Huanglongbing (HLB). With no resistant commercial citrus varieties or curable chemicals currently available, HLB remains the top threat to the world citrus industry. In this paper, two dynamic models of citrus HLB are proposed based on the preference and diffusion of citrus psyllids. The first model is a single-patch model of HLB with vector preference. The basic reproduction number of the model is calculated, and dynamic properties of the single-patch model, including the existence and local stability of the disease-free equilibrium, are analyzed. By sensitivity analysis, the parameters that have a significant impact on the basic reproduction number are identified. Numerical simulations are conducted to demonstrate that the preference of citrus psyllids is not conducive to disease prevention. Considering the diffusion of citrus psyllids between two patches, a two-patch diffusion model of HLB with preference is formulated. The global basic reproduction number of the diffusion model is determined, and the global stability of the disease-free equilibrium is established under certain conditions. Finally, numerical simulation results explore how the preference behavior of the vector and the coupling strength between two patches affect the HLB transmission.

Keywords: Citrus Huanglongbing; Preference; Diffusion; Basic reproduction number; Global stability

1 Introduction

Citrus fruits, known as the world's largest fruit, are extensively grown in diverse regions and countries including Europe, the Americas, Asia, and South Africa, with the exception of Antarctica [1]. The development of the citrus industry plays a crucial role in promoting rural employment and increasing farmers' income, while optimizing the agricultural industrial structure. It holds a significant position in the national economy, high-quality agricultural development, and rural revitalization, particularly in many regions of southern China [2]. However, the emergence of citrus Huanglongbing (HLB) poses significant threats to the citrus industry.

HLB has emerged as the primary disease jeopardizing the global citrus industry because of its highly destructive nature, rapid onset, fast transmission, and challenges in preven-

tion and control. The main symptoms of HLB include yellowing of branches, early fruit drop, mottled spots on leaves, and uneven fruit coloring [3]. As early as the mid-18th century, there were reports of HLB related diseases in India [4–6]. China first discovered HLB in the southern region in 1919 [7]. So far, 11 of the 19 provinces and regions cultivating citrus have suffered from HLB, and the affected area has reached 80% of the total area, with a production loss of approximately 85% of the total production [8]. Since 2012, significant outbreaks of HLB have ravaged regions like Ganzhou in Jiangxi Province, resulting in the removal of over 45 million diseased trees and causing an estimated direct economic loss exceeding 9 billion yuan [9]. Therefore, understanding the transmission rules of HLB and researching preventive measures has become a hot topic.

The Asian citrus psyllid (ACP) serves as the sole natural vector for HLB [10–12]. As a piercing-sucking insect, the pathogenic bacteria of HLB can reside within the psyllid's body. When a psyllid carrying the bacteria feeds on a healthy citrus tree, the pathogens enter the plant through its stylet, settle and reproduce within the plant [12]. Due to the adult psyllid's ability to fly up to 7 m high and transmit the disease within 5 hours of feeding, the individual insect transmission rate can reach as high as 70%–80%. Thus, the ACP exhibits characteristics such as high infectivity, rapid transmission, close spread, lifelong carriage of pathogens, and lifelong disease transmission [13]. To date, there is a lack of effective drugs and resistant varieties for the control of HLB, both domestically and internationally. The three main control measures currently implemented are the prevention and eradication of psyllids, the removal of infected trees, and the cultivation of disease-free seedlings [14]. The occurrence and spread of the ACP are closely related to the transmission and spread of HLB [3]. Therefore, the control of this psyllid becomes paramount in managing HLB [15].

In recent years, numerous scholars have employed mathematical models to analyze the epidemiology of HLB, with the aim of controlling disease outbreaks. However, these models have all assumed that the vector, the ACP, randomly selects host plants. In fact, existing research has demonstrated that there is a preference of the ACP towards different host plants [16]. The study by Mann et al. [17] indicates that the ACP exhibits an initial predilection for feeding on diseased plants rather than healthy ones. However, once it has consumed from an infected plant, it displays a subsequent preference for uninfected, healthy plants [12]. In other words, the preference for infected or uninfected host plants depends on whether the vector is carrying the virus or not. Citrus psyllids that are vectors of the virus demonstrate a predilection for uninfected plants, while those not harboring the virus tend to prefer infected plants. This behavior is widely recognized as the 'conditional preference' exhibited by the vector [18, 19]. These studies are of considerable scientific importance for uncovering innovative methods to combat HLB, highlighting the critical need to employ mathematical models for a thorough investigation into how the host selection behavior of psyllids influences disease spread.

In recent decades, there has been extensive attention given to the study of infectious disease models regarding the vector's preference for host selection. In 1987, Kingsolver [20] explored the impact of mosquito feeding preferences on the transmission of disease within the framework of a malaria transmission model. They improved the model by replacing the constant biting rate with a biting function that takes into account the vector's preferential selection of infected hosts. Ultimately, it was conclusively shown that the vector's preferences for selecting hosts can significantly modify the dynamics of the model.

In 2013, Buonomo et al. [21] proposed a malaria transmission model that incorporates vector's preferences and analyzed the dynamical properties of the model, obtaining the basic reproduction number. In 2018, Gandon et al. [22] established a theoretical framework to study the epidemiology and evolution of the manipulation of host choice behavior of vectors, discussing the diversity of vector behavior in the transmission of diseases between animals and plants. In 2021, Cunniffe et al. [23] enhanced the generalized model for vector-borne disease dynamics by exploring the influence of vector preference, such as landing, resting, and feeding, on the spread of plant diseases within the same host. The numerical results indicated that preferences of vectors for landing and feeding have an impact on the basic reproduction number and ultimate incidence rate of the disease. Failure to consider vector preferences would underestimate the risk of disease transmission.

Population diffusion is a widespread phenomenon observed in both the natural world and human society, with significant implications for disease spread within populations. In everyday life, diseases can easily spread from one location to another when populations frequently move between different areas. Furthermore, population dispersal can either assist in eradicating a disease, escalate its spread, or even lead to the emergence of new endemic diseases when isolated patches interact [24–34]. Hethcote [27] proposed an epidemic model with population dispersal between two patches. Brauer and van den Driessche [26] proposed a model with immigration of infective individuals. Ruxton [29] proposed a model with density-dependent migration. Jin [34] studied the effect of population dispersal among n patches on the spread of a disease.

However, there are few studies on the impact of citrus psyllid diffusion on HLB disease, and scholars have not yet considered the mathematical modeling issue of vector preferences for various citrus tree individuals. This paper introduces a dynamic HLB model that incorporates psyllid's preferences, explores the influence of preference behavior on disease transmission, and offers a fresh perspective for developing innovative strategies for controlling HLB. Based on the citrus psyllid's preference and diffusion behavior, this paper constructs both a single-patch model and a two-patch diffusion model for the spread of HLB. For the single-patch spread model, the basic reproduction number is calculated, and the dynamic properties of the model are discussed. Numerical simulations verify that citrus psyllid preference hinders disease control. In the two-patch diffusion model, a dwell time matrix couples the two patches, and the global basic reproduction number is obtained, discussing the conditions required for global stability of the disease-free equilibrium. Finally, the paper explores the influence of the citrus psyllid's preference and diffusion behavior on the trend of disease transmission.

This paper is organized as follows. In Sect. 2, a single-patch model of citrus HLB with preference is formulated, the basic reproduction number of the model is calculated, dynamic properties of the single-patch model including existence and local stability of the disease-free equilibrium are analyzed, and through sensitivity analysis, the parameters which have great influence on the basic reproduction number are obtained, and the numerical simulation are carried out to illustrate that the preference of citrus psyllid is not conducive to the prevention of disease. In Sect. 3, a two-patch diffusion model of HLB with preference is formulated, the global basic reproduction number of the diffusion model is given, and the global stability of disease-free equilibrium is proved under certain conditions, and the numerical simulation results show that the influence of preference and

diffusion of citrus psyllid on disease transmission between two patches. Finally, the conclusions with some discussion are given in Sect. 4.

2 The dynamic analysis of single-patch model

2.1 Model formulation of single-patch model

Based on the concept of compartment modeling, we adopt the *SI* model to describe the populations of citrus trees and citrus psyllids. The citrus tree population is divided into two compartments: susceptible S_h and infected I_h. Similarly, the psyllid population is divided into susceptible psyllids S_v and infected psyllids I_v compartments. Furthermore, N_h and N_v represent the total number of citrus trees and psyllids, respectively, where $N_h = S_h + I_h$ and $N_v = S_v + I_v$. According to the transmission mechanism of citrus HLB, we make the following basic assumptions:

(A1) According to the planting scale of citrus trees in the orchard, we assume that the orchard adopts an immediate replanting strategy, which means that new trees are immediately planted after symptomatic or dead trees are removed to ensure the total number of citrus trees in the orchard remains unchanged.

(A2) Considering two control measures: spraying insecticides and removing infected trees, we assume that θ represents the mortality rate of ACP due to exposure to pesticides, and d represents the rate of removal of infected trees.

(A3) If we do not consider the psyllid's host preference behavior, the number of newly infected citrus trees and psyllids in a unit of time can be assumed as follows (see [23]):

$$\phi\gamma\frac{S_h}{S_h+I_h}I_v \text{ and } \phi\eta\frac{I_h}{S_h+I_h}S_v,$$

respectively. Here, ϕ represents the average number of citrus trees visited by each citrus psyllid in a unit of time, γ represents the probability of successful virus transmission when susceptible citrus trees are fed upon by infected psyllids, η represents the probability of successful virus acquisition when susceptible psyllids feed on infected citrus trees, and $\frac{S_h}{S_h+I_h}$ and $\frac{I_h}{S_h+I_h}$ represent the probabilities of each citrus psyllid visiting susceptible and infected citrus trees, respectively.

(A4) Assume that Λ represents the constant input rate of susceptible citrus psyllids, while μ_h and μ_v represent the natural mortality rates of citrus trees and citrus psyllids, respectively.

Based on the aforementioned assumptions, we present the following HLB transmission model without considering the vector preference:

$$\begin{cases} \frac{\mathrm{d}S_h(t)}{\mathrm{d}t} = \mu_h N_h(t) + dI_h(t) - \phi\gamma\frac{S_h(t)}{S_h(t)+I_h(t)}I_v(t) - \mu_h S_h(t), \\ \frac{\mathrm{d}I_h(t)}{\mathrm{d}t} = \phi\gamma\frac{S_h(t)}{S_h(t)+I_h(t)}I_v(t) - \mu_h I_h(t) - dI_h(t), \\ \frac{\mathrm{d}S_v(t)}{\mathrm{d}t} = \Lambda - \phi\eta\frac{I_h(t)}{S_h(t)+I_h(t)}S_v(t) - \mu_v S_v(t) - \theta S_v(t), \\ \frac{\mathrm{d}I_v(t)}{\mathrm{d}t} = \phi\eta\frac{I_h(t)}{S_h(t)+I_h(t)}S_v(t) - \mu_v I_v(t) - \theta I_v(t). \end{cases} \tag{1}$$

The citrus psyllid is an insect with piercing-sucking mouthparts, using its slender stylet to penetrate citrus leaf tissue and extract nutritious sap [12]. Through behavioral observa-

tions, the psyllid's feeding behavior can be divided into three stages based on its duration of stay on the leaves: the range-searching stage, probing and piercing stage, and the resting and feeding stage. The psyllid also exhibits certain preferences for citrus trees in different states during the feeding stage [16]. We mainly focus on studying the landing, settling, and feeding tendencies of the psyllid on citrus trees with varying health conditions, as well as the impact of psyllid's feeding probability on model dynamics and the transmission control of HLB. To this end, we assume that $\bar{\nu}$ ($\tilde{\nu}$) represents the landing tendency of susceptible (infected) psyllids on infected citrus trees, $\bar{\epsilon}$ ($\tilde{\epsilon}$) represents the settling and feeding tendencies of susceptible (infected) psyllids on infected citrus trees, and $\bar{\omega}$ ($\tilde{\omega}$) represents the probability of susceptible (infected) psyllids settling and feeding on susceptible citrus trees.

First, let us consider the landing preference of citrus psyllids. It is evident that the expressions $\frac{S_h}{S_h+\bar{\nu}I_h}$, $\frac{S_h}{S_h+\tilde{\nu}I_h}$, $\frac{\bar{\nu}I_h}{S_h+\bar{\nu}I_h}$, and $\frac{\tilde{\nu}I_h}{S_h+\tilde{\nu}I_h}$ represent the probabilities of susceptible psyllids landing on susceptible trees, infected psyllids landing on susceptible trees, susceptible psyllids landing on infected trees, and infected psyllids landing on infected trees, respectively. Clearly, having $\bar{\nu} > 1$ ($\tilde{\nu} > 1$) indicates that susceptible (infected) psyllids are more prone to choose infected trees for landing. Conversely, having $\bar{\nu} < 1$ ($\tilde{\nu} < 1$) suggests that susceptible (infected) psyllids prefer healthy trees for landing.

From the aforementioned assumptions, $\bar{\omega}$, $1-\bar{\omega}$, $\tilde{\omega}$, and $1-\tilde{\omega}$ represent respectively the probabilities of susceptible psyllids residing and feeding on susceptible trees, susceptible psyllids not residing and feeding on susceptible trees, infected psyllids residing and feeding on susceptible trees, and infected psyllids not residing and feeding on susceptible trees.

Next, let us consider the habitat and feeding preferences of citrus psyllids, denoted as $\bar{\epsilon}$ and $\tilde{\epsilon}$, respectively. It is evident that $\bar{\epsilon}\bar{\omega}$, $1-\bar{\epsilon}\bar{\omega}$, $\tilde{\epsilon}\tilde{\omega}$, and $1-\tilde{\epsilon}\tilde{\omega}$ represent the probabilities of susceptible psyllids feeding on infected trees, not feeding on infected trees, infected psyllids feeding on infected trees, and infected psyllids not feeding on infected trees, respectively. Here, $\bar{\epsilon} > 1$ ($\tilde{\epsilon} > 1$) indicates a preference of susceptible (infected) psyllids for feeding on infected trees, while $\bar{\epsilon} < 1$ ($\tilde{\epsilon} < 1$) indicates a preference of susceptible (infected) psyllids for feeding on healthy trees. Let Γ represent the duration of psyllid feeding experiences, where the probing phase can be considered instantaneous compared to the feeding phase. Therefore, the average time each susceptible psyllid spends visiting a susceptible tree and an infected tree can be given by

$$\Delta_{--} = \bar{\omega}\Gamma + (1-\bar{\omega})0 = \bar{\omega}\Gamma \quad \text{and} \quad \Delta_{-+} = \bar{\epsilon}\bar{\omega}\Gamma + (1-\bar{\epsilon}\bar{\omega})0 = \bar{\epsilon}\bar{\omega}\Gamma.$$

Hence, we can derive that the average period for each susceptible psyllid to visit a citrus tree is

$$\Delta_{-} = \frac{S_h}{S_h+\bar{\nu}I_h}\bar{\omega}\Gamma + \frac{\bar{\nu}I_h}{S_h+\bar{\nu}I_h}\bar{\omega}\bar{\epsilon}\Gamma = \frac{\bar{\omega}\Gamma(S_h+\bar{\nu}\bar{\epsilon}I_h)}{S_h+\bar{\nu}I_h}.$$

Similarly, we can obtain that the average period of each infected psyllid to visit a citrus tree is

$$\Delta_{+} = \frac{S_h}{S_h+\tilde{\nu}I_h}\tilde{\omega}\Gamma + \frac{\tilde{\nu}I_h}{S_h+\tilde{\nu}I_h}\tilde{\omega}\tilde{\epsilon}\Gamma = \frac{\tilde{\omega}\Gamma(S_h+\tilde{\nu}\tilde{\epsilon}I_h)}{S_h+\tilde{\nu}I_h}.$$

If we take into account the preferences behavior of psyllids, the average numbers of visits per unit of time to citrus trees by each infected psyllid and each susceptible psyllid are

$$\tilde{\phi} = \frac{S_h + \tilde{\nu} I_h}{\tilde{\omega}\Gamma(S_h + \tilde{\nu}\tilde{\epsilon} I_h)} \text{ and } \bar{\phi} = \frac{S_h + \bar{\nu} I_h}{\bar{\omega}\Gamma(S_h + \bar{\nu}\bar{\epsilon} I_h)}.$$

Moreover, since citrus psyllids transmit viruses through feeding, they must first acquire the virus before they can transmit it. Therefore, we have $\gamma = \tilde{\omega}$, $\eta = \bar{\epsilon}\bar{\omega}$. Additionally, the probability of each infected citrus psyllid visiting a susceptible citrus tree and the probability of each susceptible psyllid visiting an infected citrus tree are given by

$$\frac{S_h}{\tilde{\omega}\Gamma(S_h + \tilde{\nu}\tilde{\epsilon} I_h)} \quad \text{and} \quad \frac{\bar{\nu} I_h}{\bar{\omega}\Gamma(S_h + \bar{\nu}\bar{\epsilon} I_h)},$$

respectively.

In conclusion, the population of newly infected citrus trees per unit of time based on the behavioral tendencies of psyllids and the population of psyllids themselves are as follows:

$$\tilde{\phi}\tilde{\omega}\frac{S_h}{\tilde{\omega}\Gamma(S_h + \tilde{\nu}\tilde{\epsilon} I_h)} I_v \text{ and } \bar{\phi}\bar{\epsilon}\bar{\omega}\frac{\bar{\nu} I_h}{\bar{\omega}\Gamma(S_h + \bar{\nu}\bar{\epsilon} I_h)} S_v,$$

that is,

$$\tilde{\phi}\frac{S_h}{\Gamma(S_h + \tilde{\nu}\tilde{\epsilon} I_h)} I_v \text{ and } \bar{\phi}\bar{\epsilon}\frac{\bar{\nu} I_h}{\Gamma(S_h + \bar{\nu}\bar{\epsilon} I_h)} S_v. \tag{2}$$

From equations (1) and (2), we establish the following model for the propagation of citrus HLB single patches based on psyllid-driven behavior:

$$\begin{cases} \frac{\mathrm{d}S_h(t)}{\mathrm{d}t} = \mu_h N_h(t) + d I_h(t) - \tilde{\phi}\frac{S_h(t)}{\Gamma\left(S_h(t) + \tilde{\nu}\tilde{\epsilon} I_h(t)\right)} I_v(t) - \mu_h S_h(t), \\ \frac{\mathrm{d}I_h(t)}{\mathrm{d}t} = \tilde{\phi}\frac{S_h(t)}{\Gamma\left(S_h(t) + \tilde{\nu}\tilde{\epsilon} I_h(t)\right)} I_v(t) - \mu_h I_h(t) - d I_h(t), \\ \frac{\mathrm{d}S_v(t)}{\mathrm{d}t} = \Lambda - \bar{\phi}\bar{\epsilon}\frac{\bar{\nu} I_h(t)}{\Gamma\left(S_h(t) + \bar{\nu}\bar{\epsilon} I_h(t)\right)} S_v(t) - \mu_v S_v(t) - \theta S_v(t), \\ \frac{\mathrm{d}I_v(t)}{\mathrm{d}t} = \bar{\phi}\bar{\epsilon}\frac{\bar{\nu} I_h(t)}{\Gamma\left(S_h(t) + \bar{\nu}\bar{\epsilon} I_h(t)\right)} S_v(t) - \mu_v I_v(t) - \theta I_v(t). \end{cases} \tag{3}$$

The symbols Λ, μ_h, μ_v, d, and θ are defined in system (1), and system (3) satisfies the initial conditions:

$$S_h(0) > 0, \quad I_h(0) \geq 0, \quad S_v(0) \geq 0, \quad I_v(0) \geq 0.$$

From the first two equations of system (3), it is evident that $\frac{\mathrm{d}N_h(t)}{\mathrm{d}t} = \frac{\mathrm{d}(S_h(t)+I_h(t))}{\mathrm{d}t} = 0$. We assume the orchard scale is constant K, that is, $N_h(t) \equiv K$. Furthermore, from the last two

equations of system (3), we can deduce that $\frac{dN_v(t)}{dt} = \frac{d(S_v(t)+I_v(t))}{dt} = \Lambda - (\mu_v + \theta)N_v(t)$. Clearly, we have

$$\limsup_{t\to\infty} N_v(t) \le \frac{\Lambda}{\mu_v + \theta}.$$

Define

$$\Omega = \left\{(S_h, I_h, S_v, I_v) \in R_+^4 |\ N_h(t) = K,\ N_v(t) \le \tfrac{\Lambda}{\mu_v+\theta}\right\}.$$

Clearly, Ω is a positive invariant set of system (3).

2.2 Existence and stability of the disease-free equilibrium

In this section, we aim to demonstrate the existence of the disease-free equilibrium, compute the basic reproduction number, and analyze the stability of the disease-free equilibrium. By simple computation, we have the disease-free equilibrium $E_0 = (S_h^0, 0, S_v^0, 0) = (K, 0, \frac{\Lambda}{\mu_v+\theta}, 0)$. The stability of the disease-free equilibrium E_0 depends on the basic reproduction number of system (3) at that point. This section utilizes the second-generation matrix method proposed by Driessche and Watmough [35] to calculate the basic reproduction number. For system (3), the matrix for the addition of new infections for the disease is denoted as F_1 and the matrix for disease transitions is denoted as V_1:

$$F_1 = \begin{pmatrix} 0 & \frac{1}{\tilde{\omega}\Gamma^2} \\ \frac{\Lambda\bar{\epsilon}\bar{\nu}}{K\bar{\omega}\Gamma^2(\mu_v+\theta)} & 0 \end{pmatrix} \text{ and } V_1 = \begin{pmatrix} \mu_h + d & 0 \\ 0 & \mu_v + \theta \end{pmatrix}. \tag{4}$$

Thus, we can determine the basic reproduction number of the system as

$$R_0 = \rho(F_1 V_1^{-1}) = \sqrt{\frac{\Lambda\bar{\epsilon}\bar{\nu}}{K\bar{\omega}\tilde{\omega}\Gamma^4(\mu_v+\theta)^2(\mu_h+d)}} = \frac{1}{\Gamma^2(\mu_v+\theta)}\sqrt{\frac{\Lambda\bar{\epsilon}\bar{\nu}}{K\bar{\omega}\tilde{\omega}(\mu_h+d)}}. \tag{5}$$

The term $\rho(F_1V_1^{-1})$ denotes the spectral radius of the second-generation generator matrix $F_1V_1^{-1}$.

Remark 2.1 From equation (5), it can be inferred that the basic reproduction number R_0 is independent of the parameters $\tilde{\nu}$ and $\tilde{\epsilon}$.

In epidemiology, the basic reproduction number, denoted by R_0, is a crucial parameter used to measure the transmission potential of infectious diseases. Consequently, according to Theorem 2 in the literature [36], the following conclusion regarding the stability of system (3) at the disease-free equilibrium E_0 can be derived.

Theorem 2.1 *When $R_0 < 1$, the disease-free equilibrium E_0 of system (3) is locally asymptotically stable; when $R_0 > 1$, the disease-free equilibrium E_0 is unstable.*

2.3 Sensitivity analysis

The model (3) integrates a variety of parameters, each with its own unique biological significance, collectively shaping the dynamics of the disease's spread through their diverse

Table 1 The parameter values of the single patch model (3)

Parameter	Description	Baseline values	Unit	Reference
K	Environmental carrying capacity of citrus trees	2000	–	[37]
Λ	Birth rate of ACP	924	day^{-1}	[37]
Γ	Feeding time of ACP	18	day^{-1}	Assumed
$\bar{\epsilon}$	Preference of susceptible ACP to inhabit and feed on infected citrus trees	1.6	–	Assumed
$\tilde{\epsilon}$	Preference of infected ACP to inhabit and feed on infected citrus trees	1.6	–	Assumed
$\bar{\upsilon}$	Susceptible ACP preference for landing on infected citrus trees	2	–	Assumed
$\tilde{\upsilon}$	Preference of infected ACP for landing on infected citrus trees	2	–	Assumed
$\bar{\omega}$	Probability of predation of susceptible ACP on susceptible citrus trees	0.5	–	[23]
$\tilde{\omega}$	The probability of infected ACP inhabiting and feeding on susceptible citrus trees	0.5	–	[23]
μ_h	Natural mortality rate of citrus tree	0.00011	day^{-1}	[37]
μ_v	Natural mortality rate of ACP	0.026	day^{-1}	[37]
θ	Mortality rate of ACP due to exposure to pesticides	0.3	day^{-1}	[37]
d	The roguing rate of infected citrus trees	0.04	day^{-1}	Assumed

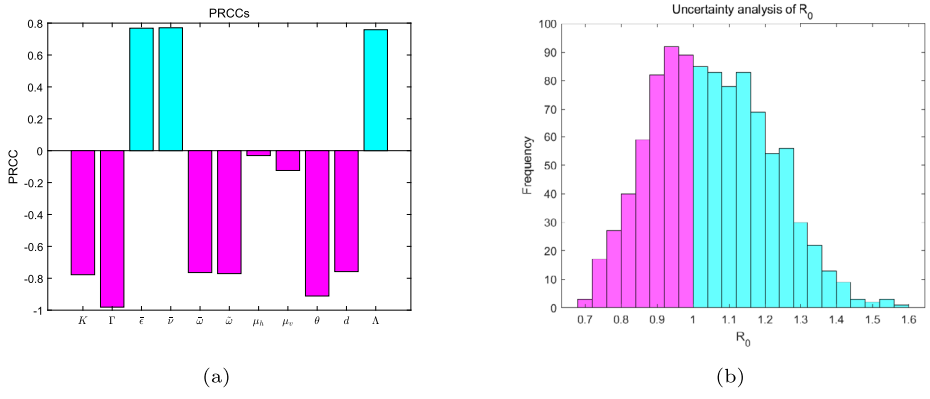

Figure 1 Sensitivity analysis and uncertainty analysis of the basic reproduction number R_0: (a) the sensitivity indices of R_0 and (b) histogram obtained from LHS using a sample size of 1000 for R_0

impacts. In this section, we will utilize Matlab software to conduct a sensitivity analysis of the model's uncertain parameters in relation to the basic reproduction number R_0 by calculating partial rank correlation coefficients (PRCC). The magnitudes of these PRCCs indicate the sensitivity of each parameter, with values closer to 1 or −1 denoting stronger sensitivity. Additionally, the sign of the PRCC signifies whether the parameter is positively or negatively correlated with R_0.

Selecting parameters, we let $\Gamma = 6$, while the values of other parameters are listed in Table 1. From the results of sensitivity analysis, it can be observed from Fig. 1(a) that R_0 is positively correlated with parameters Λ, $\bar{\epsilon}$, and $\bar{\upsilon}$, while being negatively correlated with parameters K, Γ, $\bar{\omega}$, $\tilde{\omega}$, μ_h, μ_v, θ, and d. This indicates that increasing the values of μ_h and μ_v, as well as decreasing the values of $\bar{\epsilon}$ and $\bar{\upsilon}$, can effectively reduce R_0, which contributes to the control of HLB epidemic. In particular, among all the parameters, Γ and θ exert the greatest impact on R_0, while μ_h has the least impact. The sensitivity of these parameters

provides potential intervention strategies for reducing HLB. During the HLB outbreak, extending the feeding duration of ACP on citrus trees is recommended. This strategy reduces the frequency at which each psyllid visits different trees, diminishing the likelihood of contact between psyllids and citrus trees, and consequently, decreasing the risk of HLB transmission. Additionally, stringent control measures should be enforced to regulate the population of ACP, thereby effectively managing the spread of HLB in orchards. For uncertainty analysis, we can seen from Fig. 1(b) that about 60.7% of the distribution of R_0 is greater than 1. This implies that persistent HLB bacterial infection is likely to occur.

2.4 Numerical simulation

In this section, we will evaluate the preference behavior of the citrus psyllid and the feeding probability of the psyllid on susceptible citrus trees using numerical simulations with Matlab. We are interested in studying the impact of these factors on the basic reproduction number R_0 and the final disease incidence rate $\frac{I_\infty}{S_\infty+I_\infty}$. The parameter values are presented in Table 1. For this purpose, we discuss the following two scenarios based on the objectives of this section.

Figure 2 illustrates the numerical simulation when there is no distinction between the preference behavior and feeding probability of the susceptible psyllids and infected psyllids, i.e., $\tilde{\nu} = \bar{\nu} = \nu$, $\tilde{\epsilon} = \bar{\epsilon} = \epsilon$, $\tilde{\omega} = \bar{\omega} = \omega$. The results show that the value of R_0 increases with the increase of psyllid landing preference ν and habitat feeding preference ϵ (Figs. 2(a) and 2(b)), indicating that the preference behavior of the psyllids is unfavorable for disease control. When ω is small, R_0 becomes extremely sensitive, and thereafter, it decreases with

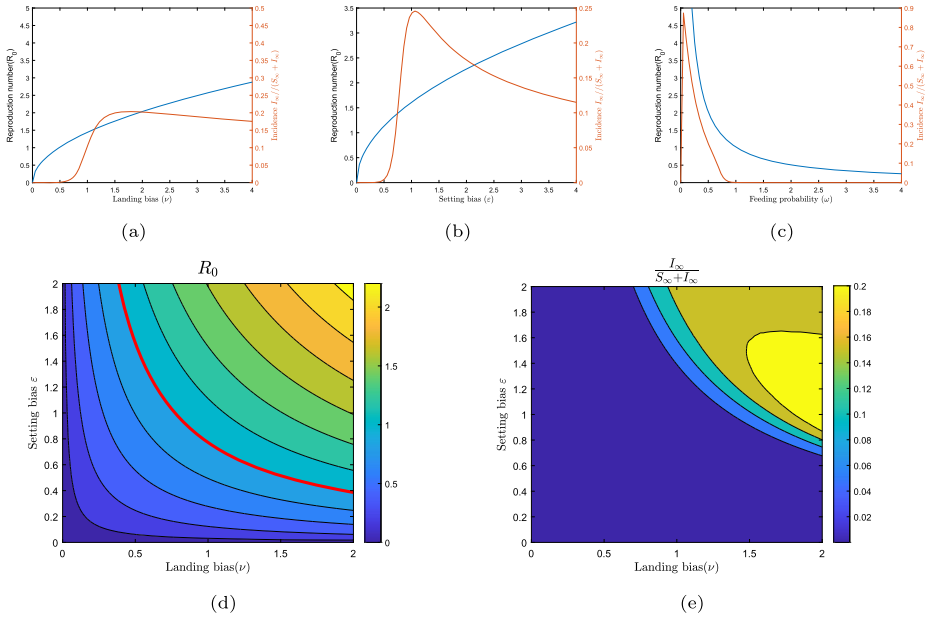

Figure 2 The basic reproduction number R_0 and the final disease incidence rate $\frac{I_\infty}{S_\infty+I_\infty}$, as well as their dependence on the parameters ν, ϵ and ω, without distinguishing between susceptible and infectious psyllids. (a) The impact of parameter ν on R_0 and $\frac{I_\infty}{S_\infty+I_\infty}$. (b) The impact of parameter ϵ on R_0 and $\frac{I_\infty}{S_\infty+I_\infty}$. (c) The impact of parameter ω on R_0 and $\frac{I_\infty}{S_\infty+I_\infty}$. (d) The contour graph of R_0 as a function of parameters ν and ϵ. The points on the red line correspond to R_0 equal to 1. (e) The contour graph of $\frac{I_\infty}{S_\infty+I_\infty}$ as a function of parameters ν and ϵ

the increase of ω (Fig. 2(c)). This indicates that increasing the feeding probability of citrus psyllids on susceptible trees is beneficial for disease control. Furthermore, the final disease incidence rate $\frac{I_\infty}{S_\infty+I_\infty}$ is nonmonotonic with respect to the parameters of psyllid landing preference ν, habitat feeding preference ϵ, and feeding probability ω. Figures 2(d) and 2(e) present contour plots of the basic reproduction number R_0 and the final disease incidence rate $\frac{I_\infty}{S_\infty+I_\infty}$ when varying the parameters ϵ and ν.

Figure 3 represents the numerical simulation graph for distinguishing between susceptible psyllids and infected psyllids in their behavior preference. The parameters $\bar{\nu}$ and $\tilde{\epsilon}$ respectively denote the landing preference of susceptible psyllids and infected psyllids on infected trees, while the parameters $\bar{\epsilon}$ and $\tilde{\epsilon}$ represent the habitat and feeding preference of susceptible psyllids and infected psyllids on infected trees. The results show that the basic reproduction number R_0 does not vary with the landing preference parameter ($\tilde{\nu}$) of infected psyllids on infected trees or the habitat and feeding preference parameter ($\tilde{\epsilon}$) of infected psyllids. However, the basic reproduction number R_0 increases with the increase in the landing preference parameter ($\bar{\nu}$) of susceptible psyllids on infected trees and the habitat and feeding preference parameter ($\bar{\epsilon}$) of susceptible psyllids (Figs. 3(a) and 3(b)). This result is consistent with the expression of R_0 and indicates that the behavior preference of susceptible psyllids towards infected citrus trees hinders the control of HLB. Meanwhile, when the parameters $\tilde{\nu}$ and $\tilde{\epsilon}$ are less than 1, the final incidence rate of the disease in the host, $\frac{I_\infty}{S_\infty+I_\infty}$, remains insensitive. However, as the parameters $\bar{\nu}$ and $\bar{\epsilon}$ increase, it is evident that the incidence rate of citrus trees in the orchard increases due to the landing and habitat and feeding preference of susceptible psyllids. This becomes a major obstacle in controlling HLB. Conversely, the final incidence rate of the disease in the host, $\frac{I_\infty}{S_\infty+I_\infty}$, decreases with the increase of parameters $\tilde{\nu}$ and $\tilde{\epsilon}$. Hence, enhancing the behavior preference of infected psyllids towards infected trees is beneficial in preventing the occurrence and spread of the disease. Figures 3(c)–3(h) show the contour plots of the final incidence rate of the disease in the host, $\frac{I_\infty}{S_\infty+I_\infty}$, as it varies with the parameters $\bar{\nu}$ and $\tilde{\nu}$, $\bar{\nu}$ and $\tilde{\epsilon}$, $\bar{\nu}$ and $\bar{\epsilon}$, as well as $\bar{\nu}$ and $\tilde{\epsilon}$.

3 The dynamic analysis of dual patch diffusion model

3.1 Model formulation of dual patch diffusion model

In this section, we will examine the spread of HLB in a heterogeneous environment characterized by two distinct patches. Let us consider patch-1 as a well-maintained orchard, whereas patch-2 denotes a neglected orchard. In the sections that follow, we intend to examine the dispersal patterns of the psyllid population and explore how psyllid behavior influences the dynamics of citrus HLB transmission.

Let $N_{hi}(t)$ and $N_{vi}(t)$ be the total number of citrus trees and psyllids in patch i ($i = 1, 2$) at time t, then $N_{hi}(t) = S_{hi}(t) + I_{hi}(t)$ and $N_{vi}(t) = S_{vi}(t) + I_{vi}(t)$. We introduce a matrix of residence times [38], denoted as P, to link the two distinct patches, where

$$P = \begin{pmatrix} p_{11} & p_{12} \\ p_{21} & p_{22} \end{pmatrix},$$

with the elements, denoted as p_{ij}, within the matrix P reflecting the proportion of time that citrus psyllids stay in patch j compared to patch i. Hence, the values of p_{ij} fall within the interval $[0, 1]$, with the constraint that $\sum_{j=1}^{2} p_{ij} = 1$, for $i = 1, 2$. It is important to note that

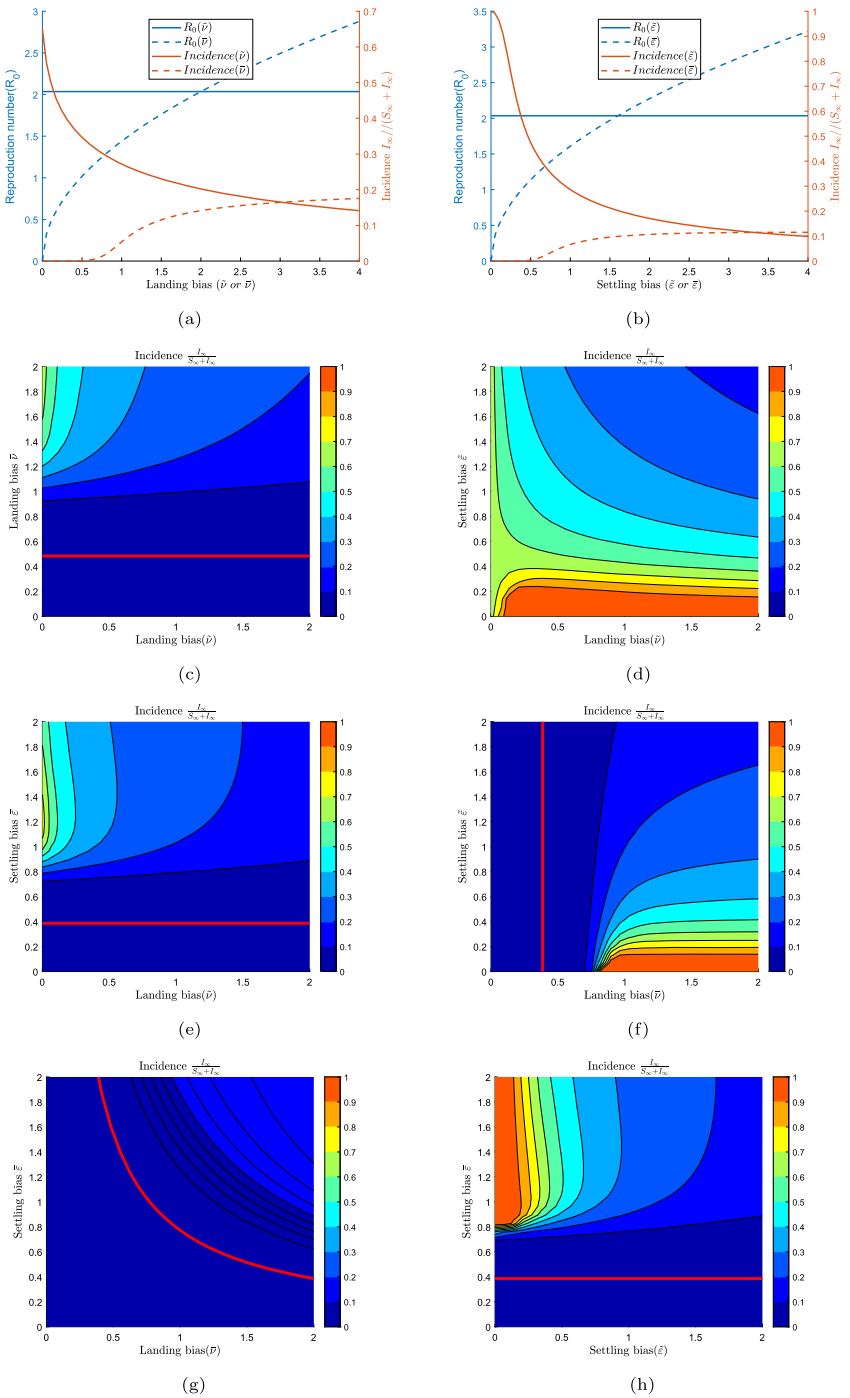

Figure 3 The basic reproduction number R_0 and the final disease incidence rate $\frac{I_\infty}{S_\infty+I_\infty}$ as well as their dependence on the parameters $\bar{\nu}$, $\tilde{\nu}$, $\bar{\epsilon}$ and $\tilde{\epsilon}$, when distinguishing between susceptible and infectious psyllids. (a) The impact of parameter $\bar{\nu}$ or $\tilde{\nu}$ on R_0 and $\frac{I_\infty}{S_\infty+I_\infty}$. (b) The impact of parameter $\bar{\epsilon}$ or $\tilde{\epsilon}$ on R_0 and $\frac{I_\infty}{S_\infty+I_\infty}$. (c) The contour graph of $\frac{I_\infty}{S_\infty+I_\infty}$ as a function of parameters $\bar{\nu}$ and $\tilde{\nu}$. The points on the red line correspond to R_0 equal to 1. (d) The contour graph of $\frac{I_\infty}{S_\infty+I_\infty}$ as a function of parameters $\tilde{\epsilon}$ and $\tilde{\nu}$. Note that R_0 does not depend on parameters $\tilde{\epsilon}$ and $\tilde{\nu}$. (e) The contour graph of $\frac{I_\infty}{S_\infty+I_\infty}$ as a function of parameters $\bar{\epsilon}$ and $\tilde{\nu}$. The points on the red line correspond to R_0 equal to 1. (f) The contour graph of $\frac{I_\infty}{S_\infty+I_\infty}$ as a function of parameters $\tilde{\epsilon}$ and $\bar{\nu}$. The points on the red line correspond to R_0 equal to 1. (g) The contour graph of $\frac{I_\infty}{S_\infty+I_\infty}$ as a function of parameters $\bar{\epsilon}$ and $\bar{\nu}$. The points on the red line correspond to R_0 equal to 1. (h) The contour graph of $\frac{I_\infty}{S_\infty+I_\infty}$ as a function of parameters $\tilde{\epsilon}$ and $\bar{\epsilon}$. The points on the red line correspond to R_0 equal to 1

in the natural environment, citrus trees do not move between patches. Only citrus psyllids have the ability to disperse between the two patches. Since susceptible trees in patch i can be infected by vectors from both patch i and disease-carrying psyllids from patch j, the average number of infected psyllids visiting citrus trees in patch i per unit time is

$$\tilde{\phi}_i = \frac{S_{hi} + \tilde{\nu}_i I_{hi}}{\tilde{\omega}_i \Gamma(S_{hi} + \tilde{\nu}_i \tilde{\epsilon}_i I_{hi})}.$$

The probability that each infected citrus psyllid visits a susceptible citrus tree in patch i is

$$\frac{S_{hi}}{\tilde{\omega}_i \Gamma(S_{hi} + \tilde{\nu}_i \tilde{\epsilon}_i I_{hi})}.$$

Similarly, susceptible psyllids in patch i can acquire the virus when they come into contact with infected citrus trees. Therefore, the average number of citrus trees visited by susceptible psyllids in patch i per unit time is

$$\bar{\phi}_i = \frac{S_{hi} + \bar{\nu}_i I_{hi}}{\bar{\omega}_i \Gamma(S_{hi} + \bar{\nu}_i \bar{\epsilon}_i I_{hi})}.$$

Furthermore, the probability of susceptible psyllids visiting infected trees in patch i is

$$\frac{\bar{\nu}_i I_{hi}}{\bar{\omega}_i \Gamma(S_{hi} + \bar{\nu}_i \bar{\epsilon}_i I_{hi})}.$$

Hence, the number of newly infected citrus tree and citrus psyllid per unit time is given by

$$\tilde{\phi}_1 \frac{S_{h1}}{\Gamma(S_{h1} + \tilde{\nu}_1 \tilde{\epsilon}_1 I_{h1})}(p_{11} I_{v1} + p_{21} I_{v2})$$

and

$$\Big(p_{11} \bar{\phi}_1 \bar{\epsilon}_1 \frac{\bar{\nu}_1 I_{h1}}{\Gamma(S_{h1} + \bar{\nu}_1 \bar{\epsilon}_1 I_{h1})} + p_{12} \bar{\phi}_2 \bar{\epsilon}_2 \frac{\bar{\nu}_2 I_{h2}}{\Gamma(S_{h2} + \bar{\nu}_2 \bar{\epsilon}_2 I_{h2})}\Big) S_{v1}.$$

The number of newly infected citrus tree and citrus psyllid per unit of time is as follows:

$$\tilde{\phi}_2 \frac{S_{h2}}{\Gamma(S_{h2} + \tilde{\nu}_2 \tilde{\epsilon}_2 I_{h2})}(p_{12} I_{v1} + p_{22} I_{v2})$$

and

$$\Big(p_{21} \bar{\phi}_1 \bar{\epsilon}_1 \frac{\bar{\nu}_1 I_{h1}}{\Gamma(S_{h1} + \bar{\nu}_1 \bar{\epsilon}_1 I_{h1})} + p_{22} \bar{\phi}_2 \bar{\epsilon}_2 \frac{\bar{\nu}_2 I_{h2}}{\Gamma(S_{h2} + \bar{\nu}_2 \bar{\epsilon}_2 I_{h2})}\Big) S_{v2}.$$

Based on the above discussions and assumptions, we formulate the following diffusion model of citrus HLB, characterized by two patches:

$$\begin{cases} \dfrac{\mathrm{d}S_{hi}(t)}{\mathrm{d}t} = \mu_{hi}N_{hi}(t) + d_iI_{hi}(t) - \tilde{\phi}_i\dfrac{S_{hi}(t)}{\Gamma\left(S_{hi}(t)+\tilde{\nu}_i\tilde{\epsilon}_iI_{hi}(t)\right)}\left(\sum_{j=1}^{2}p_{ji}I_{vj}(t)\right) - \mu_{hi}S_{hi}(t), \\ \dfrac{\mathrm{d}I_{hi}(t)}{\mathrm{d}t} = \tilde{\phi}_i\dfrac{S_{hi}(t)}{\Gamma\left(S_{hi}(t)+\tilde{\nu}_i\tilde{\epsilon}_iI_{hi}(t)\right)}\left(\sum_{j=1}^{2}p_{ji}I_{vj}(t)\right) - \mu_{hi}I_{hi}(t) - d_iI_{hi}(t), \\ \dfrac{\mathrm{d}S_{vi}(t)}{\mathrm{d}t} = \Lambda_i - S_{vi}(t)\left(\sum_{j=1}^{2}p_{ij}\bar{\phi}_j\bar{\epsilon}_j\dfrac{\bar{\nu}_jI_{hj}(t)}{\Gamma\left(S_{hj}(t)+\bar{\nu}_j\bar{\epsilon}_jI_{hj}(t)\right)}\right) - \mu_{vi}S_{vi}(t) - \theta_iS_{vi}(t), \\ \dfrac{\mathrm{d}I_{vi}(t)}{\mathrm{d}t} = S_{vi}(t)\left(\sum_{j=1}^{2}p_{ij}\bar{\phi}_j\bar{\epsilon}_j\dfrac{\bar{\nu}_jI_{hj}(t)}{\Gamma\left(S_{hj}(t)+\bar{\nu}_j\bar{\epsilon}_jI_{hj}(t)\right)}\right) - \mu_{vi}I_{vi}(t) - \theta_iI_{vi}(t). \end{cases} \tag{6}$$

The subscripts i ($i = 1, 2$) are used to distinguish between the two patches, and the model parameters have the same meanings as those in the single patch model (3). The system (6) satisfies the initial conditions:

$$S_{hi}(0) \geq 0, \quad I_{hi}(0) \geq 0, \quad S_{vi}(0) \geq 0, \quad I_{vi}(0)) \geq 0. \tag{7}$$

3.2 Analysis of the dynamics of model (6)

In this section, we will study the threshold dynamics of the diffusion model with two patches (6). For the convenience of subsequent discussions, we denote

$$N_H(t) = N_{h1}(t) + N_{h2}(t), \qquad N_V(t) = N_{v1}(t) + N_{v2}(t),$$
$$\Lambda_V = 2\max\{\Lambda_1, \Lambda_2\}, \qquad \mu_V(t) = \min\{\mu_{v1} + \theta_1, \mu_{v2} + \theta_2\}.$$

Adding the first two equations of system (6), we obtain

$$\frac{\mathrm{d}N_{hi}(t)}{\mathrm{d}t} \equiv 0, \quad i = 1, 2. \tag{8}$$

This means that the number of citrus fruit plantations in the orchard remains constant. We assume that the sizes of Orchard 1 and Orchard 2 are denoted as K_1 and K_2, respectively. Consequently, we can derive $N_H(t) = N_{h1}(t) + N_{h2}(t) = K_1 + K_2$. Thus, we define the set as follows:

$$\Theta = \left\{(S_{h1}, I_{h1}, S_{v1}, I_{v1}, S_{h2}, I_{h2}, S_{v2}, I_{v2}) \in R_+^8 \,|\, N_H(t) = K_1 + K_2,\ N_V(t) \leq \tfrac{\Lambda_V}{\mu_V}\right\}.$$

3.3 The nonnegativity and boundedness of the solution

Theorem 3.1 *Let $x(t) = (S_{h1}(t), I_{h1}(t), S_{v1}(t), I_{v1}(t), S_{h2}(t), I_{h2}(t), S_{v2}(t), I_{v2}(t))$ be the solution of system (6) with initial values (7). Then, for $t \geq 0$, the components of $x(t)$ are nonnegative and bounded. The set Θ is a forward invariant set of system (6).*

Proof First, we demonstrate the nonnegativity of the solution. Since both initial values of the host and vector populations are nonnegative, the right-hand side of the system (6) is continuous on the set Θ and satisfies a local Lipschitz condition. According to [39], it is known that the system (6) has a unique solution on the interval $[0, \tau)$, where $0 < \tau \leq +\infty$. Suppose the solution of the model is negative, then there exists a first time $\hat{t} > 0$ such that

$$\begin{aligned}\hat{t} = \inf \{t \mid {} & S_{h1}(t) = 0 \text{ or } I_{h1}(t) = 0 \text{ or } S_{v1}(t) = 0 \text{ or } I_{v1}(t) = 0 \text{ or } S_{h2}(t) = 0 \\ & \text{or } I_{h2}(t) = 0 \text{ or } S_{v2}(t) = 0 \text{ or } I_{v2}(t) = 0\}.\end{aligned}$$

If $S_{h1}(\hat{t}) = 0$, then we have $S_{v1}(t) > 0$, $S_{h1}(t) > 0$, $I_{h1}(t) > 0$, $I_{v1}(t) > 0$, $S_{h2}(t) > 0$, $I_{h2}(t) > 0$, $S_{v2}(t) > 0$, $I_{v2}(t) > 0$, for $t \in (0, \hat{t})$. It is obvious that $\frac{\mathrm{d}S_{v1}(\hat{t})}{\mathrm{d}t} < 0$. From the third equation of system (6), we obtain

$$\frac{\mathrm{d}S_{v1}(\hat{t})}{\mathrm{d}t} = \Lambda_1 > 0.$$

This is a contradiction. Hence, for all $t \geq 0$, it follows that $S_{v1}(t) \geq 0$. Similarly, we can obtain that for all $t \geq 0$, $S_{h1}(t) \geq 0$, $I_{h1}(t) \geq 0$, $I_{v1}(t) \geq 0$, $S_{h2}(t) \geq 0$, $I_{h2}(t) \geq 0$, $S_{v2}(t) \geq 0$, and $I_{v2}(t) \geq 0$. Therefore, for all $t \geq 0$, we have $x(t) \geq 0$.

Next, we demonstrate the boundedness of the solution. By adding the last two equations of the system (6), we have the differential equation $\frac{\mathrm{d}N_{vi}(t)}{\mathrm{d}t} = \Lambda_i - (\mu_{vi} + \theta_i)N_{vi}(t)$. This implies that, as $t \to \infty$, $N_{vi}(t) \to \frac{\Lambda_i}{\mu_{vi}+\theta_i}$ for $i = 1, 2$. Hence, $\frac{\mathrm{d}N_V(t)}{\mathrm{d}t} = \frac{\mathrm{d}N_{v1}(t)}{\mathrm{d}t} + \frac{\mathrm{d}N_{v2}(t)}{\mathrm{d}t} = \Lambda_1 + \Lambda_2 - (\mu_{v1} + \theta_1)N_{v1}(t) - (\mu_{v2} + \theta_2)N_{v2}(t) \leq 2\max\{\Lambda_1, \Lambda_2\} - \min\{\mu_{v1} + \theta_1, \mu_{v2} + \theta_2\}N_V(t) = 2\Lambda_V - \mu_V N_V(t)$. Thus, as $t \to \infty$, $\limsup_{t\to+\infty} N_V(t) \to \frac{\Lambda_V}{\mu_V}$, indicating that $N_V(t)$ is bounded. Therefore, the set Θ is a forward invariant set for the system (6). □

Next, we shall delve into the examination of the nonnegativity and boundedness of the solution to the provided model (6).

3.4 The disease-free equilibrium and the basic reproduction number

In the diffusion model, there are four infection terms, namely I_{h1}, I_{v1}, I_{h2}, and I_{v2}. Let all the infection terms be equal to zero, i.e., $I_{h1}(t) = I_{v1}(t) = I_{h2}(t) = I_{v2}(t) = 0$. Then the disease-free equilibrium can be represented as

$$E^0 = \left(S_{h1}^0, 0, S_{v1}^0, 0, S_{h2}^0, 0, S_{v2}^0, 0\right) = \left(K_1, 0, \frac{\Lambda_1}{\mu_{v1} + \theta_1}, 0, K_2, 0, \frac{\Lambda_2}{\mu_{v2} + \theta_2}, 0\right).$$

In order to analyze the stability of the system (6), it is necessary to obtain the threshold condition for HLB. By utilizing the method of the next generation matrix defined in [35], we can determine the basic reproduction number R_0 of the system (6). Based on the model (6), the additional infection term $\mathcal{F}$ and the transition term $\mathcal{V}$ are given as follows:

$$\mathcal{F} = \begin{pmatrix} \tilde{\phi}_1 \left(p_{11} I_{v1} + p_{21} I_{v2}\right) \dfrac{S_{h1}}{\Gamma(S_{h1} + \tilde{\nu}_1 \tilde{\epsilon}_1 I_{h1})} \\ S_{v1} \left(p_{11} \bar{\phi}_1 \bar{\epsilon}_1 \dfrac{\bar{\nu}_1 I_{h1}}{\Gamma(S_{h1} + \bar{\nu}_1 \bar{\epsilon}_1 I_{h1})} + p_{12} \bar{\phi}_2 \bar{\epsilon}_2 \dfrac{\bar{\nu}_2 I_{h2}}{\Gamma(S_{h2} + \bar{\nu}_2 \bar{\epsilon}_2 I_{h2})} \right) \\ \tilde{\phi}_2 \left(p_{12} I_{v1} + p_{22} I_{v2}\right) \dfrac{S_{h2}}{\Gamma(S_{h2} + \tilde{\nu}_2 \tilde{\epsilon}_2 I_{h2})} \\ S_{v2} \left(p_{21} \bar{\phi}_1 \bar{\epsilon}_1 \dfrac{\bar{\nu}_1 I_{h1}}{\Gamma(S_{h1} + \bar{\nu}_1 \bar{\epsilon}_1 I_{h1})} + p_{22} \bar{\phi}_2 \bar{\epsilon}_2 \dfrac{\bar{\nu}_2 I_{h2}}{\Gamma(S_{h2} + \bar{\nu}_2 \bar{\epsilon}_2 I_{h2})} \right) \end{pmatrix},$$

$$\mathcal{V} = \begin{pmatrix} (\mu_{h1} + d_1)I_{h1} \\ (\mu_{v1} + \theta_1)I_{v1} \\ (\mu_{h2} + d_2)I_{h2} \\ (\mu_{v2} + \theta_2)I_{v2} \end{pmatrix}.$$

The matrix for the addition of new infections, denoted as F_2, and the matrix for disease transitions, denoted as V_2, are calculated as:

$$F_2 = \begin{pmatrix} 0 & \frac{p_{11}}{\tilde{\omega}_1\Gamma^2} & 0 & \frac{p_{21}}{\tilde{\omega}_1\Gamma^2} \\ \frac{p_{11}\bar{\epsilon}_1\bar{\nu}_1}{K_1\bar{\omega}_1\Gamma^2}S_{v1}^0 & 0 & \frac{p_{12}\bar{\epsilon}_2\bar{\nu}_2}{K_2\bar{\omega}_2\Gamma^2}S_{v1}^0 & 0 \\ 0 & \frac{p_{12}}{\tilde{\omega}_2\Gamma^2} & 0 & \frac{p_{22}}{\tilde{\omega}_2\Gamma^2} \\ \frac{p_{21}\bar{\epsilon}_1\bar{\nu}_1}{K_1\bar{\omega}_1\Gamma^2}S_{v2}^0 & 0 & \frac{p_{22}\bar{\epsilon}_2\bar{\nu}_2}{K_2\bar{\omega}_2\Gamma^2}S_{v2}^0 & 0 \end{pmatrix}, \tag{9}$$

$$V_2 = \begin{pmatrix} \mu_{h1} + d_1 & 0 & 0 & 0 \\ 0 & \mu_{v1} + \theta_1 & 0 & 0 \\ 0 & 0 & \mu_{h2} + d_2 & 0 \\ 0 & 0 & 0 & \mu_{v2} + \theta_2 \end{pmatrix}. \tag{10}$$

A simple computation yields

$$F_2V_2^{-1} = \begin{pmatrix} 0 & \frac{p_{11}}{\tilde{\omega}_1\Gamma^2(\mu_{v1} + \theta_1)} & 0 & \frac{p_{21}}{\tilde{\omega}_1\Gamma^2(\mu_{v2} + \theta_2)} \\ \frac{p_{11}\bar{\epsilon}_1\bar{\nu}_1S_{v1}^0}{K_1\bar{\omega}_1\Gamma^2(\mu_{h1} + d_1)} & 0 & \frac{p_{12}\bar{\epsilon}_2\bar{\nu}_2S_{v1}^0}{K_2\bar{\omega}_2\Gamma^2(\mu_{h2} + d_2)} & 0 \\ 0 & \frac{p_{12}}{\tilde{\omega}_2\Gamma^2(\mu_{v1} + \theta_1)} & 0 & \frac{p_{22}}{\tilde{\omega}_2\Gamma^2(\mu_{v2} + \theta_2)} \\ \frac{p_{21}\bar{\epsilon}_1\bar{\nu}_1S_{v2}^0}{K_1\bar{\omega}_1\Gamma^2(\mu_{h1} + d_1)} & 0 & \frac{p_{22}\bar{\epsilon}_2\bar{\nu}_2S_{v2}^0}{K_2\bar{\omega}_2\Gamma^2(\mu_{h2} + d_2)} & 0 \end{pmatrix}.$$

Hence, the expression for the global basic reproduction number of the diffusion model (6) is given by

$$\widetilde{R}_0 = \rho(F_2V_2^{-1}) = \sqrt{\frac{\varphi_1 + \sqrt{\varphi_2}}{2}},$$

where $\rho(F_2V_2^{-1})$ denotes the spectral radius of the matrix $F_2V_2^{-1}$, and

$$\begin{aligned} \varphi_1 &= \frac{p_{11}^2\bar{\epsilon}_1\bar{\nu}_1\Lambda_1}{K_1\bar{\omega}_1\tilde{\omega}_1\Gamma^4(\mu_{v1} + \theta_1)^2(\mu_{h1} + d_1)} + \frac{p_{21}^2\bar{\epsilon}_1\bar{\nu}_1\Lambda_2}{K_1\bar{\omega}_1\tilde{\omega}_1\Gamma^4(\mu_{v2} + \theta_2)^2(\mu_{h1} + d_1)} \\ &\quad + \frac{p_{22}^2\bar{\epsilon}_2\bar{\nu}_2\Lambda_2}{K_2\bar{\omega}_2\tilde{\omega}_2\Gamma^4(\mu_{v2} + \theta_2)^2(\mu_{h2} + d_2)} + \frac{p_{12}^2\bar{\epsilon}_2\bar{\nu}_2\Lambda_1}{K_2\bar{\omega}_2\tilde{\omega}_2\Gamma^4(\mu_{v1} + \theta_1)^2(\mu_{h2} + d_2)}, \\ \varphi_2 &= \varphi_1^2 - 4\left[\frac{\bar{\epsilon}_1\bar{\nu}_1\bar{\epsilon}_2\bar{\nu}_2\Lambda_1\Lambda_2(p_{11}p_{22} - p_{12}p_{21})^2}{K_1K_2\bar{\omega}_1\tilde{\omega}_1\bar{\omega}_2\tilde{\omega}_2\Gamma^8(\mu_{v1} + \theta_1)^2(\mu_{v2} + \theta_2)^2(\mu_{h1} + d_1)(\mu_{h2} + d_2)}\right] > 0. \end{aligned}$$

Remark 3.2. When the two patches are uncoupled, i.e., $p_{11} = 1$ and $p_{22} = 1$, the local basic reproduction numbers of the two patches can be obtained as follows:

$$R_{01} = \sqrt{\frac{\bar{\epsilon}_1 \bar{\nu}_1 \Lambda_1}{K_1 \tilde{\omega}_1 \tilde{\omega}_1 \Gamma^4 (\mu_{\nu 1} + \theta_1)^2 (\mu_{h1} + d_1)}}, \quad R_{02} = \sqrt{\frac{\bar{\epsilon}_2 \bar{\nu}_2 \Lambda_2}{K_2 \tilde{\omega}_2 \tilde{\omega}_2 \Gamma^4 (\mu_{\nu 2} + \theta_2)^2 (\mu_{h2} + d_2)}}.$$

Remark 3.3. The above φ_1 and φ_2 can be expressed using R_{01} and R_{02}, respectively, that is,

$$\varphi_1 = R_{01}^2 (p_{11}^2 + p_{21}^2 \frac{\Lambda_2 (\mu_{\nu 1} + \theta_1)^2}{\Lambda_1 (\mu_{\nu 2} + \theta_2)^2}) + R_{02}^2 \left(p_{22}^2 + p_{12}^2 \frac{\Lambda_1 (\mu_{\nu 2} + \theta_2)^2}{\Lambda_2 (\mu_{\nu 1} + \theta_1)^2} \right),$$

$$\varphi_2 = \varphi_1^2 - 4 R_{01}^2 R_{02}^2 (p_{11} p_{22} - p_{12} p_{21})^2.$$

The overall basic reproduction number, $\tilde{R}_0$, is related to two local basic reproduction numbers, R_{01} and R_{02}.

Next, let us discuss the local asymptotic stability of the equilibrium point E^0 and present the following theorem.

Theorem 3.2 *If $\widetilde{R}_0 < 1$, then the disease-free equilibrium E^0 of the bistable system (6) is locally asymptotically stable, whereas E^0 is unstable if $\widetilde{R}_0 > 1$.*

Theorem 3.2 illustrates that, when $\widetilde{R}_0 < 1$, the presence of a few infected individuals will not lead to a widespread epidemic. In order to eradicate the disease without relying on the initial number of infected individuals, it is imperative to discuss the global stability of the disease-free equilibrium.

3.5 The global stability of the disease-free equilibrium

Here we discuss the global stability of the disease-free equilibrium E^0 using the methods proposed by Castillo-Chavez et al. [40].

Theorem 3.3 *If $\widetilde{R}_0 < 1$ and $\tilde{\epsilon}_1 \geq 0.5$, $\tilde{\epsilon}_2 \geq 0.5$, $\bar{\epsilon}_1 > 1$, $\bar{\nu}_1 > 1$, $\bar{\epsilon}_2 > 1$, $\bar{\nu}_2 > 1$, the disease-free equilibrium E^0 of the bistable system is globally asymptotically stable.*

Proof System (6) can be rewritten as follows:

$$\begin{aligned} \frac{\mathrm{d}X}{\mathrm{d}t} &= F(X, Y), \\ \frac{\mathrm{d}Y}{\mathrm{d}t} &= G(X, Y), \quad G(X, \mathbf{0}) = 0. \end{aligned} \tag{11}$$

The vector $X = (S_{h1}(t), S_{\nu 1}(t), S_{h2}(t), S_{\nu 2}(t)) \in \mathbb{R}^4$ represents the uninfected compartments in system (6), while $Y = (I_{h1}(t), I_{\nu 1}(t), I_{h2}(t), I_{\nu 2}(t)) \in \mathbb{R}^4$ represents the infected compartments in the system (6). The disease-free equilibrium is $E^0 = (X^*, \mathbf{0})$, given the initial state $X^* = (S_{h1}^0, S_{\nu 1}^0, S_{h2}^0, S_{\nu 2}^0) = (K_1, \frac{\Lambda_1}{\mu_{\nu 1} + \theta_1}, K_2, \frac{\Lambda_2}{\mu_{\nu 2} + \theta_2})$, with $\mathbf{0}$ denoting the zero vector. Global stability of the disease-free equilibrium can be proven when the following two conditions hold:

($H1$) For the differential equation $\frac{\mathrm{d}X}{\mathrm{d}t} = F(X, \mathbf{0})$, X^* is globally asymptotically stable.

$(H2)$ $G(X,Y)$ can be rewritten as $A^*Y - \hat{G}(X,Y)$, where the matrix A^* is defined as $D_Y(X^*,\mathbf{0})$, an M matrix. Additionally, it holds that $\hat{G}(X,Y) \geq 0$ for all $X, Y \in \Theta$.

It is evident from equation (6) that $X = (S_{h1}, S_{v1}, S_{h2}, S_{v2})$ and $Y = (I_{h1}, I_{v1}, I_{h2}, I_{v2})$. Therefore, we can conclude that

$$F(X,Y) = \begin{pmatrix} \mu_{h1}N_{h1} + d_1 I_{h1} - \tilde{\phi}_1(\sum_{j=1}^{2} p_{j1} I_{vj}) \dfrac{S_{h1}}{\Gamma(S_{h1} + \tilde{\nu}_1 \tilde{\epsilon}_1 I_{h1})} - \mu_{h1} S_{h1} \\ \Lambda_1 - S_{v1}(\sum_{j=1}^{2} p_{1j} \bar{\phi}_j \bar{\epsilon}_j \dfrac{\bar{\nu}_j I_{hj}}{\Gamma(S_{hj} + \bar{\nu}_j \bar{\epsilon}_j I_{hj})}) - (\mu_{v1} + \theta_1) S_{v1} \\ \mu_{h2}N_{h2} + d_2 I_{h2} - \tilde{\phi}_2(\sum_{j=1}^{2} p_{j2} I_{vj}) \dfrac{S_{h2}}{\Gamma(S_{h2} + \tilde{\nu}_2 \tilde{\epsilon}_2 I_{h2})} - \mu_{h2} S_{h2} \\ \Lambda_2 - S_{v2}(\sum_{j=1}^{2} p_{1j} \bar{\phi}_j \bar{\epsilon}_j \dfrac{\bar{\nu}_j I_{hj}}{\Gamma(S_{hj} + \bar{\nu}_j \bar{\epsilon}_j I_{hj})}) - (\mu_{v2} + \theta_2) S_{v2} \end{pmatrix}.$$

Consider the equilibrium point in the absence of any disturbances, denoted as $E^0 = (X^*, \mathbf{0})$, thus

$$F(X,\mathbf{0}) = \begin{pmatrix} \mu_{h1}K_1 - \mu_{h1}S_{h1} \\ \Lambda_1 - (\mu_{v1} + \theta_1) S_{v1} \\ \mu_{h2}K_2 - \mu_{h2}S_{h2} \\ \Lambda_2 - (\mu_{v2} + \theta_2) S_{v2} \end{pmatrix}.$$

It is evident that, as $t \to \infty$,

$$S_{h1}(t) \to K_1, \ \ S_{v1}(t) \to \frac{\Lambda_1}{\mu_{v1} + \theta_1}, \ \ S_{h2} \to K_2, \ \ S_{v2}(t) \to \frac{\Lambda_2}{\mu_{v2} + \theta_2}.$$

Given that $\lim_{t\to\infty} X(t) = X^*$, when $\widetilde{R}_0 < 1$, the subsystem $\frac{\mathrm{d}X(t)}{\mathrm{d}t} = F(X,\mathbf{0})$ has a globally asymptotically stable equilibrium point $X^* = (K_1, \frac{\Lambda_1}{\mu_{v1}+\theta_1}, K_2, \frac{\Lambda_2}{\mu_{v2}+\theta_2})$, satisfying condition $(H1)$.

Next, we aim to demonstrate that, for $(X,Y) \in \Theta$, we have $\hat{G}(X,Y) \geq 0$. In fact,

$$G(X,Y) = \begin{pmatrix} \tilde{\phi}_1(\sum_{j=1}^{2} p_{j1} I_{vj}) \dfrac{S_{h1}}{\Gamma(S_{h1} + \tilde{\nu}_1 \tilde{\epsilon}_1 I_{h1})} - \mu_{h1} I_{h1} - d_1 I_{h1} \\ S_{v1}(\sum_{j=1}^{2} p_{1j} \bar{\phi}_j \bar{\epsilon}_j \dfrac{\bar{\nu}_j I_{hj}}{\Gamma(S_{hj} + \bar{\nu}_j \bar{\epsilon}_j I_{hj})}) - (\mu_{v1} + \theta_1) I_{v1} \\ \tilde{\phi}_2(\sum_{j=1}^{2} p_{j2} I_{vj}) \dfrac{S_{h2}}{\Gamma(S_{h2} + \tilde{\nu}_2 \tilde{\epsilon}_2 I_{h2})} - \mu_{h2} I_{h1} - d_2 I_{h2} \\ S_{v2}(\sum_{j=1}^{2} p_{2j} \bar{\phi}_j \bar{\epsilon}_j \dfrac{\bar{\nu}_j I_{hj}}{\Gamma(S_{hj} + \bar{\nu}_j \bar{\epsilon}_j I_{hj})}) - (\mu_{v2} + \theta_2) I_{v2} \end{pmatrix}.$$

By calculating, we can obtain the matrix A^* as

$$A^* = F_2 - V_2 = \begin{pmatrix} -(\mu_{h1} + d_1) & \dfrac{p_{11}}{\tilde{\omega}_1 \Gamma^2} & 0 & \dfrac{p_{21}}{\tilde{\omega}_1 \Gamma^2} \\ \dfrac{p_{11}\bar{\epsilon}_1\bar{\nu}_1}{K_1 \bar{\omega}_1 \Gamma^2} S_{v1}^0 & -(\mu_{v1} + \theta_1) & \dfrac{p_{12}\bar{\epsilon}_2\bar{\nu}_2}{K_2 \bar{\omega}_2 \Gamma^2} S_{v1}^0 & 0 \\ 0 & \dfrac{p_{12}}{\tilde{\omega}_2 \Gamma^2} & -(\mu_{h2} + d_2) & \dfrac{p_{22}}{\tilde{\omega}_2 \Gamma^2} \\ \dfrac{p_{21}\bar{\epsilon}_1\bar{\nu}_1}{K_1 \bar{\omega}_1 \Gamma^2} S_{v2}^0 & 0 & \dfrac{p_{22}\bar{\epsilon}_2\bar{\nu}_2}{K_2 \bar{\omega}_2 \Gamma^2} S_{v2}^0 & -(\mu_{v2} + \theta_2) \end{pmatrix}.$$

Hence,

$$\hat{G}(X,Y) = A^*Y - G(X,Y)$$
$$= \begin{pmatrix} \frac{p_{11}I_{v1}+p_{21}I_{v2}}{\tilde{\omega}_1\Gamma^2} - \frac{S_{h1}(S_{h1}+\tilde{\nu}_1 I_{h1})}{\tilde{\omega}_1\Gamma^2(S_{h1}+\tilde{\nu}_1\tilde{\epsilon}_1 I_{h1})^2}(p_{11}I_{v1}+p_{21}I_{v2}) \\ \frac{p_{11}\bar{\epsilon}_1\bar{\nu}_1 S^0_{v1}I_{h1}}{\bar{\omega}_1\Gamma^2} + \frac{p_{12}\bar{\epsilon}_2\bar{\nu}_2 S^0_{v1}I_{h2}}{\bar{\omega}_2\Gamma^2} - S_{v1}(\frac{p_{11}\bar{\epsilon}_1\bar{\nu}_1 I_{h1}(S_{h1}+\bar{\nu}_1 I_{h1})}{\bar{\omega}_1\Gamma^2(S_{h1}+\bar{\nu}_1\bar{\epsilon}_1 I_{h1})^2} \\ +\frac{p_{12}\bar{\epsilon}_2\bar{\nu}_2 I_{h2}(S_{h2}+\bar{\nu}_2 I_{h2})}{\bar{\omega}_2\Gamma^2(S_{h2}+\bar{\nu}_2\bar{\epsilon}_2 I_{h2})^2}) \\ \frac{p_{12}I_{v1}+p_{22}I_{v2}}{\tilde{\omega}_2\Gamma^2} - \frac{S_{h2}(S_{h2}+\tilde{\nu}_2 I_{h2})}{\tilde{\omega}_2\Gamma^2(S_{h2}+\tilde{\nu}_2\tilde{\epsilon}_2 I_{h2})^2}(p_{12}I_{v1}+p_{22}I_{v2}) \\ \frac{p_{21}\bar{\epsilon}_1\bar{\nu}_1 S^0_{v2}I_{h1}}{\bar{\omega}_1\Gamma^2} + \frac{p_{22}\bar{\epsilon}_2\bar{\nu}_2 S^0_{v2}I_{h2}}{\bar{\omega}_2\Gamma^2} \\ -S_{v2}(\frac{p_{21}\bar{\epsilon}_1\bar{\nu}_1 I_{h1}(S_{h1}+\bar{\nu}_1 I_{h1})}{\bar{\omega}_1\Gamma^2(S_{h1}+\bar{\nu}_1\bar{\epsilon}_1 I_{h1})^2} + \frac{p_{22}\bar{\epsilon}_2\bar{\nu}_2 I_{h2}(S_{h2}+\bar{\nu}_2 I_{h2})}{\bar{\omega}_2\Gamma^2(S_{h2}+\bar{\nu}_2\bar{\epsilon}_2 I_{h2})^2}) \end{pmatrix}.$$

It is evident that, in order to ensure $\hat{G}(X,Y) \geq 0$, certain conditions must be satisfied. If $\tilde{\epsilon}_1 \geq 0.5$, the first element of matrix $\hat{G}(X,Y)$ satisfies

$$\frac{(p_{11}I_{v1}+p_{21}I_{v2})(\tilde{\nu}_1^2\tilde{\epsilon}_1{}^2 I_{h1}^2 + S_{h1}I_{h1}\tilde{\nu}_1(2\tilde{\epsilon}_1-1))}{\tilde{\omega}_1\Gamma^2(S_{h1}+\tilde{\nu}_1\tilde{\epsilon}_1 I_{h1})^2} \geq 0.$$

Furthermore, if $\bar{\epsilon}_1 > 1$, $\bar{\nu}_1 > 1$, $\bar{\epsilon}_2 > 1$, and $\bar{\nu}_2 > 1$, the second element of matrix $\hat{G}(X,Y)$ satisfies

$$\frac{p_{11}\bar{\epsilon}_1\bar{\nu}_1 S^0_{v1}I_{h1}}{\bar{\omega}_1\Gamma^2} + \frac{p_{12}\bar{\epsilon}_2\bar{\nu}_2 S^0_{v1}I_{h2}}{\bar{\omega}_2\Gamma^2} - S_{v1}(\frac{p_{11}\bar{\epsilon}_1\bar{\nu}_1 I_{h1}(S_{h1}+\bar{\nu}_1 I_{h1})}{\bar{\omega}_1\Gamma^2(S_{h1}+\bar{\nu}_1\bar{\epsilon}_1 I_{h1})^2} + \frac{p_{12}\bar{\epsilon}_2\bar{\nu}_2 I_{h2}(S_{h2}+\bar{\nu}_2 I_{h2})}{\bar{\omega}_2\Gamma^2(S_{h2}+\bar{\nu}_2\bar{\epsilon}_2 I_{h2})^2})$$
$$= \frac{p_{11}\bar{\epsilon}_1\bar{\nu}_1 I_{h1}}{\bar{\omega}_1\Gamma^2}[S^0_{v1} - \frac{S_{v1}(S_{h1}+\bar{\nu}_1 I_{h1})}{(S_{h1}+\bar{\nu}_1\bar{\epsilon}_1 I_{h1})^2}] + \frac{p_{12}\bar{\epsilon}_2\bar{\nu}_2 I_{h2}}{\bar{\omega}_2\Gamma^2}[S^0_{v1} - \frac{S_{v1}(S_{h2}+\bar{\nu}_2 I_{h2})}{(S_{h2}+\bar{\nu}_2\bar{\epsilon}_2 I_{h2})^2}] \geq 0.$$

Similarly, if $\tilde{\epsilon}_2 \geq 0.5$ and $\bar{\epsilon}_1 > 1$, $\bar{\nu}_1 > 1$, $\bar{\epsilon}_2 > 1$, $\bar{\nu}_2 > 1$, it can be ensured that the third and fourth elements of the matrix $\hat{G}(X,Y)$ are greater than or equal to zero. In conclusion, when $\tilde{\epsilon}_1 \geq 0.5$, $\tilde{\epsilon}_2 \geq 0.5$, $\bar{\epsilon}_1 > 1$, $\bar{\nu}_1 > 1$, $\bar{\epsilon}_2 > 1$, and $\bar{\nu}_2 > 1$, for any $X, Y \in \Theta$, $\hat{G}(X,Y) \geq 0$. Moreover, since it is an M matrix, condition (H2) holds. Therefore, when $\widetilde{R}_0 < 1$ and $\tilde{\epsilon}_1 \geq 0.5$, $\tilde{\epsilon}_2 \geq 0.5$, $\bar{\epsilon}_1 > 1$, $\bar{\nu}_1 > 1$, $\bar{\epsilon}_2 > 1$, and $\bar{\nu}_2 > 1$, the disease-free equilibrium E^0 of the system (6) is globally asymptotically stable. □

3.6 Numerical simulation

In this section, we will assess the attributive behavior and feeding probability of citrus psyllids through numerical simulation, and examine the impact of their behavior on the spread of HLB between two patches. Additionally, we will explore the effects of varying coupling strengths on the dispersion of psyllid populations and its consequences on the system identified in equation (6).

It is noted that there exist three different coupling situations between two patches: unidirectional coupling, symmetric coupling, and asymmetric coupling. Unidirectional coupling refers to a situation where citrus psyllids can only diffuse from patch i to patch j, resulting in $p_{jj} = 1$. Symmetric coupling occurs when the residence time of citrus psyllids after diffusing from patch i to patch j is equal to the residence time after diffusing from

patch j to patch i, i.e., $p_{ij} = p_{ji}$. Conversely, asymmetric coupling occurs when the residence time of citrus psyllids after diffusing from patch i to patch j is greater than the residence time after diffusing from patch j to patch i, i.e., $p_{ij} > p_{ji}$. Additionally, diffusion can be categorized as either weak or strong based on diffusion capability. In this paper, we consider the following five coupling scenarios:

(S_1) No diffusion between patches: the two patches are isolated. The citrus psyllid in patch-1 will not spread to patch-2, and the citrus psyllid in patch-2 will also not spread to patch-1. In other words, $p_{11} = p_{22} = 1$, $p_{12} = p_{21} = 0$;

(S_2) Unidirectional weak diffusion: The citrus psyllid in patch-1 will diffuse to patch-2 weakly, while the citrus psyllid in patch-2 will not diffuse to patch-1. Let $p_{11} = 0.8$, $p_{12} = 0.2$, $p_{21} = 0$, and $p_{22} = 1$;

(S_3) Unidirectional strong diffusion: The citrus aphids in patch-1 will spread to patch-2 and exhibit strong diffusion, while the citrus aphids in patch-2 will not spread to patch-1. Let $p_{11} = 0.2$, $p_{12} = 0.8$, $p_{21} = 0$, $p_{22} = 1$;

(S_4) Bidirectional weak diffusion: The citrus psyllid in patch-1 will diffuse to patch-2, and the citrus psyllid in patch-2 will also diffuse to patch-1, both are weak diffusions. Let $p_{11} = 0.8$, $p_{12} = 0.2$, $p_{21} = 0.2$, $p_{22} = 0.8$;

(S_5) Bidirectional strong diffusion: The citrus psyllids in patch-1 will spread to patch-2, and the citrus psyllids in patch-2 will also spread to patch-1, both exhibiting strong diffusion. Let $p_{11} = 0.2$, $p_{12} = 0.8$, $p_{21} = 0.8$, and $p_{22} = 0.2$.

Due to the differences in the environment of patch-1 and patch-2, the parameters chosen for each patch are also different. The parameter values for patch-1 are shown in Table 1, while the selected parameters for patch-2 are as follows: $K_2 = 1000$, $\Lambda_2 = 462$, $\theta_2 = 0$, $d_2 = 0.02$, and the remaining parameters are the same as those for patch-1. In subsequent discussions, unless otherwise specified, we will use the aforementioned parameter values.

Figure 4 depicts the variation of the preference parameters and feeding probabilities of patch-1 and patch-2, as well as the basic reproduction number $\widetilde{R}_0$ of system (6) under five different coupling scenarios. It can be observed that the influence of preference parameters and feeding probabilities on the basic reproduction number $\widetilde{R}_0$ is consistent in the first three coupling scenarios (uncoupled, unidirectional weak diffusion, and unidirectional strong diffusion). This suggests that the threshold dynamics of the coupled system (6) are primarily determined by the diffusion from patch-1 to patch-2 and the absence of diffusion between the two patches. Furthermore, the basic reproduction number $\widetilde{R}_0$ remains unchanged with variations in the landing and habitat preferences ($\tilde{\nu}_i$, $\tilde{\epsilon}_i$, $i = 1, 2$) of the infected aphids on diseased citrus trees. On the other hand, it increases with an increase in the landing and habitat preferences ($\bar{\nu}_i$, $\bar{\epsilon}_i$, $i = 1, 2$) of susceptible aphids on infected citrus trees, and decreases as the feeding probability ($\bar{\omega}_i$, $\tilde{\omega}_i$, $i = 1, 2$) of susceptible and infected aphids on susceptible citrus trees increases. Additionally, Figs. 4(a)–4(f) demonstrate that the basic reproduction number is minimized under strong diffusion intensity, followed by weak diffusion intensity, and maximized when there is no diffusion between the two patches. This suggests that increasing the dispersion intensity of the citrus psyllid between patch-1 and patch-2 is advantageous for the control of citrus HLB disease.

Figure 5 depicts the influence of different coupling strengths and diffusion coefficients on the basic reproduction number $\widetilde{R}_0$, when R_{01} varies with a fixed value of R_{02}. We assume that patch-2 is the neglected orchard, and patch-1 is the well-managed orchard. Here,

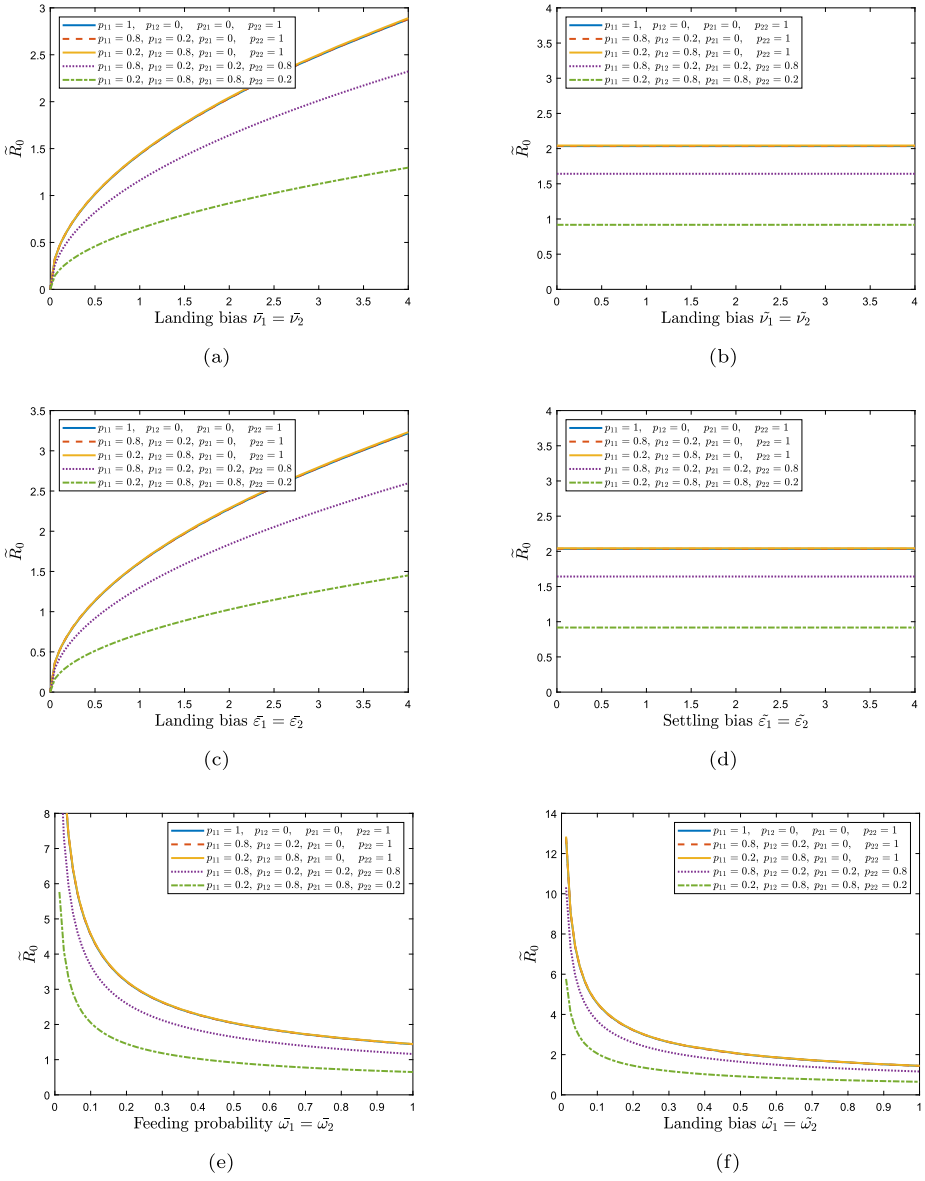

Figure 4 Graph of changes in the basic reproduction number, $\widetilde{R}_0$, under five different coupling scenarios: (a) when $\bar{\nu}_1=\bar{\nu}_2$, $\widetilde{R}_0$ is influenced by $\bar{\nu}_1$; (b) when $\tilde{\nu}_1=\tilde{\nu}_2$, $\widetilde{R}_0$ is influenced by $\tilde{\nu}_1$; (c) when $\bar{\epsilon}_1=\bar{\epsilon}_2$, $\widetilde{R}_0$ is influenced by $\bar{\epsilon}_1$; (d) when $\tilde{\epsilon}_1=\tilde{\epsilon}_2$, $\widetilde{R}_0$ is influenced by $\tilde{\epsilon}_1$; (e) when $\bar{\omega}_1=\bar{\omega}_2$, $\widetilde{R}_0$ is influenced by $\bar{\omega}_1$; and (f) when $\tilde{\omega}_1=\tilde{\omega}_2$, $\widetilde{R}_0$ is influenced by $\tilde{\omega}_1$

$R_{01}=0.4790$ and $R_{02}=2.0356$. It can be observed that when p_{22} takes smaller values, $\widetilde{R}_0$ decreases to less than 1 with varying p_{11}. The dependence of $\widetilde{R}_0$ on p_{11} and p_{22} in the diffusion system is nonmonotonic. Furthermore, when psyllids do not spread from patch-2 to patch-1, that is, when $p_{22}=0$, $\widetilde{R}_0$ is less than 1 for $p_{11}\in[0.1,0.8]$, while for other cases it is greater than 1. This implies that an appropriate coupling strength leads to the transition of system (6) from a uniformly persistent state to an extinct state, and coupling strength that is too strong or too weak is not conducive to disease control.

Figure 6 illustrates the impact of different preference parameters on the basic reproduction number $\widetilde{R}_0$ of the diffusion system. Here, $P_{\bar{\nu}}=\frac{\bar{\nu}}{1+\bar{\nu}}$ represents the landing preference

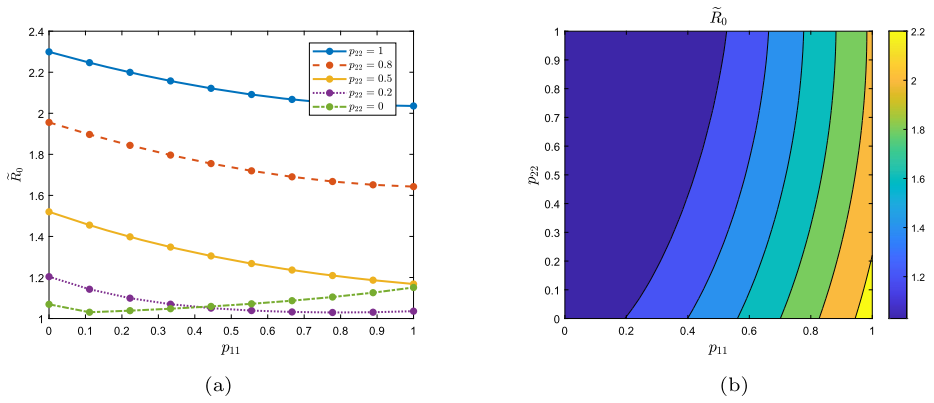

Figure 5 Investigating the impact of p_{11} and p_{22} on the fundamental reproduction number, $\widetilde{R}_0$, with $R_{01} = 0.5354$ and $R_{02} = 2.0356$: (a) the relationship between $\widetilde{R}_0$ and p_{11} under five different values of p_{22}; (b) The contour graph of $\widetilde{R}_0$ as a function of parameters p_{11} and p_{12}

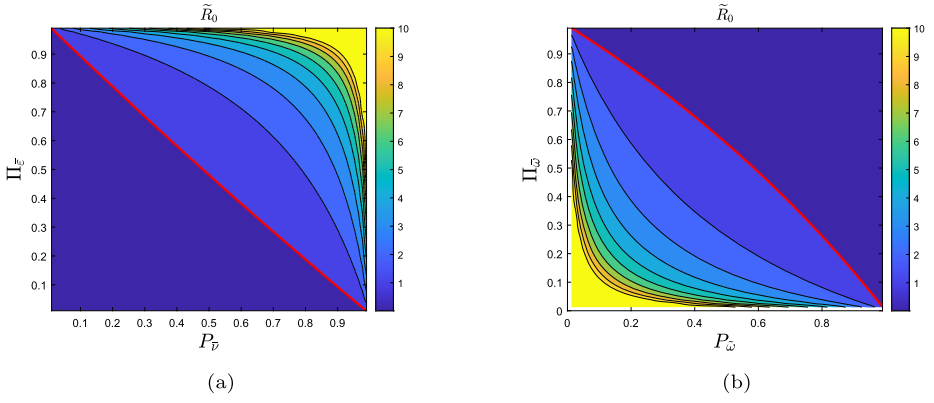

Figure 6 The influence of different preferences on the basic reproduction number, denoted as $\widetilde{R}_0$, varies: (a) the contour graph of $\widetilde{R}_0$ as a function of parameters $P_{\bar{\nu}}$ and $\Pi_{\bar{\epsilon}}$; (b) the contour graph of $\widetilde{R}_0$ as a function of parameters $P_{\tilde{\omega}}$ and $\Pi_{\tilde{\omega}}$

of susceptible psyllids on infected citrus trees, $\Pi_{\bar{\epsilon}} = \frac{\bar{\epsilon}}{1+\bar{\epsilon}}$ represents the habitat and feeding preference of susceptible psyllids on infected citrus trees, $P_{\tilde{\omega}} = \frac{\tilde{\omega}}{1+\tilde{\omega}}$ represents the feeding preference of infected psyllids on susceptible citrus trees, and $\Pi_{\bar{\omega}} = \frac{\bar{\omega}}{1+\bar{\omega}}$ represents the feeding preference of susceptible psyllids on susceptible citrus trees. It can be seen from Fig. 6 that when both $P_{\bar{\nu}}$, $\Pi_{\bar{\epsilon}}$ take smaller values, and $P_{\tilde{\omega}}$, $\Pi_{\bar{\omega}}$ take larger values simultaneously, it ensures that the basic reproduction number $\widetilde{R}_0 < 1$. Conversely, if $\widetilde{R}_0 > 1$, it indicates the opposite scenario. Therefore, reducing the landing and habitat/feeding preferences of susceptible psyllids on infected citrus trees, or increasing the feeding probabilities of susceptible psyllids on susceptible citrus trees and infected psyllids on infected citrus trees, is advantageous for controlling the spread of HLB.

4 Conclusion

Based on the preference and diffusion behavior of the ACP, we establish two dynamic models: (1) an HLB transmission model based on psyllid preference (model (3)) and (2) a diffusion model for citrus HLB based on psyllid preference (model (6)). When the HLB

is only transmitted within a single patch, we calculate the disease-free equilibrium and the basic reproduction number of model (3). We analyze the local stability of the disease-free equilibrium and conduct sensitivity analysis on the system parameters to identify the parameters that have a significant impact on the basic reproduction number R_0. Finally, through numerical simulations, we explore the effects of psyllid preference and feeding probability on R_0 and the final disease incidence ($\frac{I_\infty}{S_\infty+I_\infty}$), under two scenarios: distinguishing or not psyllid preference and feeding probability. The results show that the preference of susceptible psyllids for infected trees hinders disease control, while the preference of infected psyllids for infected trees aids in disease suppression. When the ACP disperses between two patches, assuming patch-1 represents a well-managed orchard and patch-2 represents a management-deficient orchard, we couple the two patches using residence time matrices. We calculate the basic reproduction number of the spread model (6) and prove that, under certain conditions, the disease-free equilibrium of system (6) is globally asymptotically stable. Furthermore, by some numerical simulations, we investigate the dynamic changes of the model under five different levels of coupling strength. The results suggest that increasing the dispersal strength of the ACP between the two patches facilitates disease control. Additionally, for the case of unidirectional diffusion, where psyllids only disperse from patch 1 to patch 2, appropriate diffusion will facilitate disease control, but both large- and small-scale diffusion will not be beneficial for disease control.

Acknowledgements
The research has been supported by the Natural Science Foundation of China (12361097, 12361098), the Natural Science Foundation of Jiangxi Province (20224ACB201003, 20232BAB201024), the Science and Technology Project of Education Department of Jiangxi Province (GJJ2201205), and Jiangxi Provincial Key Laboratory of Pest and Disease Control of Featured Horticultural Plants (2024SSY04181).

Author contributions
S. Gao established the model; Y. Luo and S. Tang analyzed the model; Y. Liu performed the numerical simulation; Y. Luo and S. Tang wrote the paper; F. Zhang carried out the parameter estimation. All authors have read and agreed to the published version of the manuscript.

Data availability
This research does not involve real data. No data were used, and no new data were created.

Declarations

Competing interests
The authors declare that there are no conflicts of interests regarding the publication of this paper.

Received: 18 September 2024 Accepted: 22 November 2024 Published online: 03 December 2024

References

1. Liu, Y., Heying, E., Tanumihardjo, S.A.: History, global distribution, and nutritional importance of citrus fruits. Compr. Rev. Food Sci. Food Saf. **11**(6), 530–545 (2012)
2. Qi, C., Gu, Y., Zeng, Y.: Progress of citrus industry economy in China. J. Huazhong Agric. Univ. **40**(1), 58–69 (2021)
3. Da Graça, J., Korsten, L.: Citrus Huanglongbing: Review, present status and future strategies. Diseases of Fruits and Vegetables Volume I: Diagnosis and Management, 229–245 (2004)
4. Bové, J.M.: Huanglongbing: a destructive, newly-emerging, century-old disease of citrus. J. Plant Pathol., 7–37 (2006)
5. Gottwald, T.R.: Current epidemiological understanding of citrus Huanglongbing. Annu. Rev. Phytopathol. **48**, 119–139 (2010)
6. Da Graça, J.V.: Biology, history and world status of Huanglongbing. Memorias del Taller Internacional sobre el Huanglongbing y el Psílido asiático de los cítricos, 1–7 (2008)
7. Hanson, H.C.: Diseases and pests of economic plants of central and south China, Hong Kong and Taiwan (Formosa). A study based on field survey data and on pertinent records. Material, and reports (1963)
8. Da Graça, J.V., Douhan, G.W., Halbert, S.E., Keremane, M.L., Lee, R.F., Vidalakis, G., Zhao, H.: Huanglongbing: an overview of a complex pathosystem ravaging the world's citrus. J. Integr. Plant Biol. **58**(4), 373–387 (2016)
9. Yuan, X., Chen, C., Bassanezi, R.B., Wu, F., Feng, Z., Shi, D., Li, J., Du, Y., Zhong, L., Zhong, B., et al.: Region-wide comprehensive implementation of roguing infected trees, tree replacement, and insecticide applications successfully controls citrus Huanglongbing. Phytopathology **111**(8), 1361–1368 (2021)

10. Halbert, S.E., Manjunath, K.L.: Asian citrus psyllids (Sternorrhyncha: Psyllidae) and greening disease of citrus: a literature review and assessment of risk in Florida. Fla. Entomol. **87**(3), 330–353 (2004)
11. Stelinski, L.L.: Ecological aspects of the vector-borne bacterial disease, citrus greening (Huanglongbing): dispersal and host use by Asian citrus psyllid, Diaphorina citri Kuwayama. Insects **10**(7), 208 (2019)
12. Hall, D.G., Richardson, M.L., Ammar, E.-D., Halbert, S.E.: Asian citrus psyllid, Diaphorina citri, vector of citrus Huanglongbing disease. Entomol. Exp. Appl. **146**(2), 207–223 (2013)
13. Wang, N., Trivedi, P.: Citrus Huanglongbing: a newly relevant disease presents unprecedented challenges. Phytopathology **103**(7), 652–665 (2013)
14. Alvarez, S., Rohrig, E., Solís, D., Thomas, M.H.: Citrus greening disease (Huanglongbing) in Florida: economic impact, management and the potential for biological control. Agric. Res. **5**, 109–118 (2016)
15. Sétamou, M., Sanchez, A., Patt, J.M., Nelson, S.D., Jifon, J., Louzada, E.S.: Diurnal patterns of flight activity and effects of light on host finding behavior of the Asian citrus psyllid. J. Insect Behav. **25**, 264–276 (2012)
16. Johnston, N., Stansly, P.A., Stelinski, L.L.: Secondary hosts of the Asian citrus psyllid, Diaphorina citri Kuwayama: survivorship and preference. J. Appl. Entomol. **143**(9), 921–928 (2019)
17. Mann, R.S., Ali, J.G., Hermann, S.L., Tiwari, S., Pelz-Stelinski, K.S., Alborn, H.T., Stelinski, L.L.: Induced release of a plant-defense volatile 'deceptively' attracts insect vectors to plants infected with a bacterial pathogen. PLoS Pathog. **8**(3), 1002610 (2012)
18. Zhao, J.P., Wang, H.T., Zeng, X.N., Xue, P.P.: Differences in selection behaviors and chemical cues of adult Asian citrus psyllids, Diaphorina citri, on healthy and Huanglongbing-infected young shoots of citrus plants. J. Agric. Sci. **5**(9), 83 (2013)
19. Cen, Y., Yang, C., Holford, P., Beattie, G.A.C., Spooner Hart, R.N., Liang, G., Deng, X.: Feeding behaviour of the Asiatic citrus psyllid, Diaphorina citri, on healthy and Huanglongbing-infected citrus. Entomol. Exp. Appl. **143**(1), 13–22 (2012)
20. Kingsolver, J.G.: Mosquito host choice and the epidemiology of malaria. Am. Nat. **130**(6), 811–827 (1987)
21. Buonomo, B., Vargas De León, C.: Stability and bifurcation analysis of a vector-bias model of malaria transmission. Math. Biosci. **242**(1), 59–67 (2013)
22. Gandon, S.: Evolution and manipulation of vector host choice. Am. Nat. **192**(1), 23–34 (2018)
23. Cunniffe, N.J., Taylor, N.P., Hamelin, F.M., Jeger, M.J.: Epidemiological and ecological consequences of virus manipulation of host and vector in plant virus transmission. PLoS Comput. Biol. **17**(12), 1009759 (2021)
24. Brauer, F., Castillo Chavez, C.: Mathematical Models in Population Biology and Epidemiology, vol. 2. Springer, New York (2012)
25. Hamer, W.H.: The Milroy Lectures on Epidemic Diseases in England: the Evidence of Variability and of Persistency of Type, vol. 167, pp. 569–574. Bedford Press, London (1906)
26. Brauer, F., Driessche, P.: Models for transmission of disease with immigration of infectives. Math. Biosci. **171**(2), 143–154 (2001)
27. Hethcote, H.W.: Qualitative analyses of communicable disease models. Math. Biosci. **28**(3–4), 335–356 (1976)
28. McNeill, W.: Plagues and Peoples. Anchor, New York (2010)
29. McNeill, W.: Density-dependent migration and stability in a system of linked populations. Bull. Math. Biol. **58**(4), 643–660 (1996)
30. Wang, W.: Population dispersal and disease spread. Discrete Contin. Dyn. Syst., Ser. B **4**(3), 797–804 (2004)
31. Wang, W., Mulone, G.: Threshold of disease transmission in a patch environment. J. Math. Anal. Appl. **285**(1), 321–335 (2003)
32. Wang, W., Ruan, S.: Simulating the SARS outbreak in Beijing with limited data. J. Theor. Biol. **227**(3), 369–379 (2004)
33. Wang, W., Zhao, X.Q.: An epidemic model in a patchy environment. Math. Biosci. **190**(1), 97–112 (2004)
34. Jin, Y., Wang, W.: The effect of population dispersal on the spread of a disease. J. Math. Anal. Appl. **308**(1), 343–364 (2005)
35. Driessche, P., Watmough, J.: Reproduction numbers and sub-threshold endemic equilibria for compartmental models of disease transmission. Math. Biosci. **180**(1–2), 29–48 (2002)
36. Dohm, D.J., O'Guinn, M.L., Turell, M.J.: Effect of environmental temperature on the ability of Culex pipiens (Diptera: Culicidae) to transmit West Nile virus. J. Med. Entomol. **39**(1), 221–225 (2002)
37. Liao, Z., Gao, S., Yan, S., Zhou, G.: Transmission dynamics and optimal control of a Huanglongbing model with time delay. Math. Biosci. Eng. **18**(4), 4162–4192 (2021)
38. Lee, S., Castillo-Chavez, C.: The role of residence times in two-patch Dengue transmission dynamics and optimal strategies. J. Theor. Biol. **374**, 152–164 (2015)
39. Hale, J.K.: Functional differential equations. In: Analytic Theory of Differential Equations: The Proceedings of the Conference at Western Michigan University, Kalamazoo, 30 April–2 May 1970, pp. 9–22. Springer, Berlin (2006)
40. Castillo-Chavez, C., Song, B.: Dynamical models of tuberculosis and their applications. Math. Biosci. Eng. **1**(2), 361–404 (2004)

Publisher's Note